Aggregates of Polymer-Substituted Fullerenes

Qi Liao,* Xiaozhong Qu, Liusheng Chen, and Xigao Jin

State Key Laboratory of Polymer Physics and Chemistry, Joint Laboratory of Polymer Science and Materials, Institute of Chemistry, Chinese Academy of Sciences, Beijing 100080, China

Received: November 15, 2005; In Final Form: February 21, 2006

We analyzed the self-organized supermolecular architectures observed in solutions of singly polymer-substituted fullerenes by light-scattering and fluorescence spectroscopy, as well as the surface pattern obtained from spraying the solution by atomic force microscopy. We found that the concentration dependence on aggregate size and fluorescence intensity can be explained quantitatively using a scaling argument, assuming that the aggregates in solution are self-emulsified micelles. Our results indicate that the core of the structure is unreacted fullerenes. Based on our scaling arguments, we predict that there is a critical molecular weight that allows for a narrow distribution of the self-assembled structures in solution.

1. Introduction

Since its discovery, fullerene (C_{60}) has been extensively investigated because of its unique chemical and physical properties.[1] However, potential applications are limited due to the extreme solvent-phobicity of fullerene. Researchers have attempted to modify fullerenes by grafting various polymers onto the surface in an effort to improve its poor solubility and processibility.[2−5] In this aspect, the solution behavior of polymer chains attached to fullerene, including the dispersion state (individual molecules or multi-chain aggregates) and chain conformation, directly impacts the applications of such a modified fullerene.

Recently, laser light-scattering data revealed that fullerenes grafted with linear polymer chains, such as poly(methyl methacrylate) (PMMA), poly(*n*-butyl methacrylate),[6] and poly(ethylene oxide) (PEO)[7] could form aggregates in a solvent that was selective for the polymer chains, in contrast to an expected molecularly dispersed fullerene solution. The association behavior of substituted fullerenes in solution has been extensively studied. However, the reports on such supermolecular structures are still limited to a phenomenal description. A theoretical explanation of the morphology and the concentration dependence on aggregation remains controversial.[6−9]

A simple micelle structure was first proposed[6] with the vesicle model also considered.[10,11] However, such models do not explain the following experimental observations concurrently:

(i) The size of the aggregates is one decade larger than that of the single chain and simple micelle.

(ii) The aggregate size has a negative concentration dependence, which means that its size decreases as the concentration increases. This is not explained by the simple micelle model or vesicle model for dilute polymer solutions.

(iii) The molecular weight dependence on size and distribution vary with the different polymer systems. A very narrow size distribution can be observed in most solutions,[6,7] however, broad distributions of the size distribution have also been reported[2].

The purpose of this paper is to clarify the structure of aggregates recently observed in a solution of singly polymer-grafted C_{60}, as well as to clarify the effect of molecular weight, concentration, and solvent properties on the self-assembly mechanism. In this study, three types of polymer-grafted fullerenes, that is, PMMA, polystyrene (PS), and hydrophilic PEO were studied. The hydrodynamic radii (R_h) of the self-assembled structures were investigated by dynamic light scattering (DLS). The morphology of the aggregates adsorbed on a mica surface was observed using atomic force microscopy (AFM). The concentration dependence of PS-grafted fullerenes on their aggregation properties was investigated using fluorescence spectroscopy.

2. Experimental Section

The methods for the synthesis and purification of C_{60}-containing polymers C_{60}-*g*-PMMA ($M_w = 1.1 \times 10^4$ g/mol), C_{60}-*g*-PEO ($M_w = 2000$ g/mol), and C_{60}-*g*-PS [$M_w = 2500$, 4700, and 7900 g/mol; determined by gel permeation chromatography (GPC)] is well-documented.[3−5] On average, one polymer chain was grafted to each C_{60}. Tetrahydrofuran (THF) and 1,1,2-trichloroethane (TCE) (Beijing Chemical Reagents Co.) were distilled twice prior to use.

DLS measurements were carried out on a commercial light-scattering spectrometer (ALV/SP-125) equipped with an ALV-5000 multi-τ digital time correlator and a He−Ne laser (Model 127, output power 40 mW at $\lambda = 632$ nm). The primary beam is vertically polarized with respect to the scattering plane. The solutions were filtered with a 0.2- or a 0.45-μm Millipore PTFE filter. All the DLS measurements were carried out at 25.0 ± 0.1 °C. DLS measurements give the size distribution of the aggregates in solution. Figure 1a shows the R_h distribution of C_{60}-*g*-PS with different M_w's in TCE.

Solutions with selected aggregate concentrations were sprayed onto freshly cleaved mica surfaces via a home-built sprayer and dried rapidly in a vacuum at room temperature. The surface morphology of the samples was observed using a tapping-mode atomic force microscope (Nanoscope IIIa, Digital Instruments) equipped with a silicon cantilever (TESP type, resonance frequency 250−300 kHz) in air at room temperature. AFM images of samples corresponding to different M_w solutions are shown in Figures 1b−d. Line scans show that the shapes are hemispherical.

A Hitachi F4500 fluorescence spectrophotometer was used to record the liquid surface emission and excitation spectra. Reflection fluorescence was observed with radiation at an angle

10.1021/jp056588j CCC: $33.50
Published on Web 03/17/2006

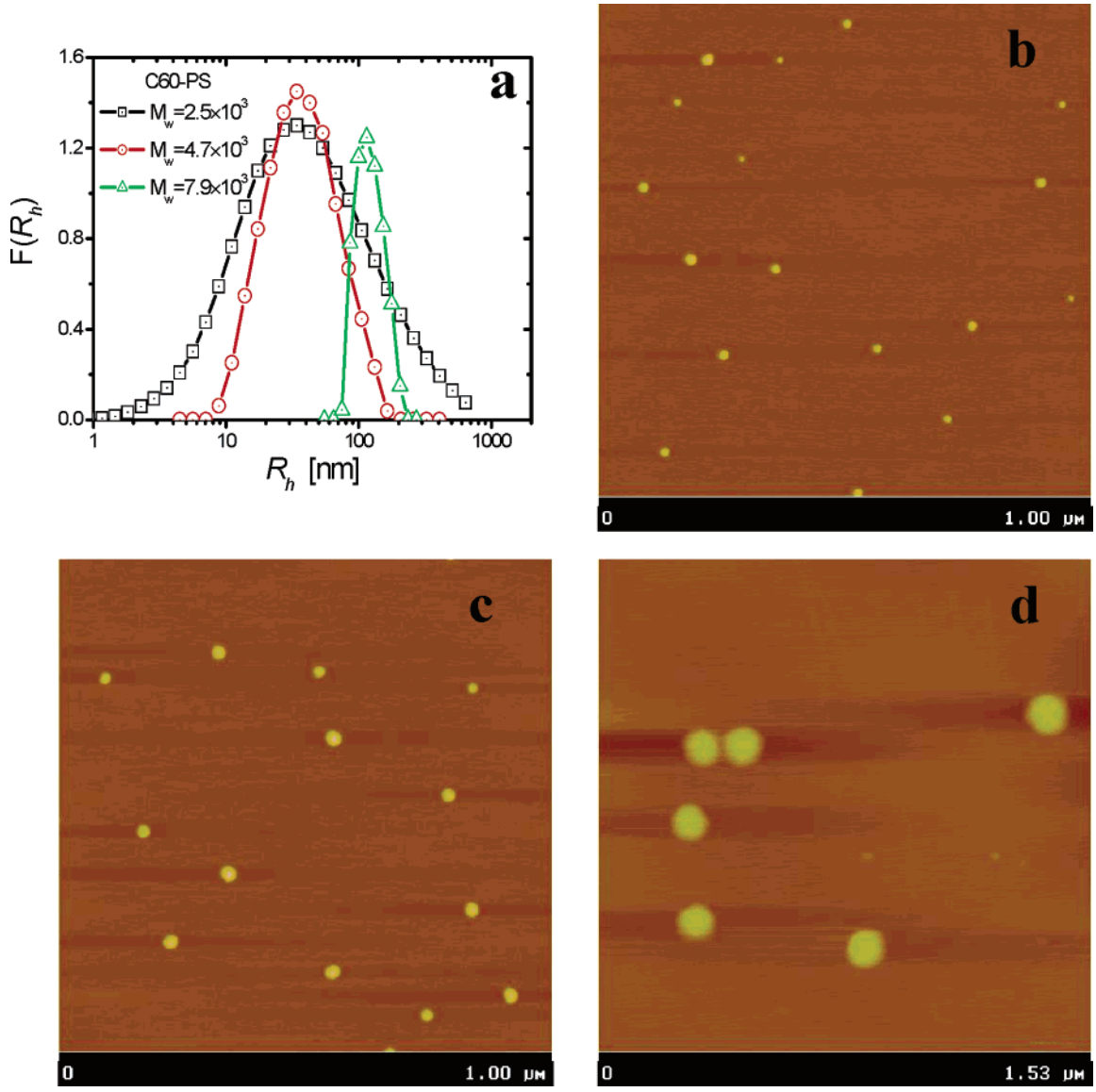

Figure 1. (a) Normalized R_h distributions of fullerenes grafted with different molecular weight PSs in TCE solution, where $T = 25$ °C and the polymer concentrations are 5.0×10^{-5} g/mL, 1.0×10^{-4} g/mL, and 1.56×10^{-4} g/mL, respectively. (b), (c), and (d) AFM images of C_{60}−PS samples sprayed and dried on mica after drying for 72 h in a vacuum with $M_w = 2.5 \times 10^3$ g/mol, 4.7×10^3 g/mol, and 7.9×10^3 g/mol, respectively.

of incidence of 30° on one of the sides of a quartzose cell containing the copolymer solution. Both the emission and the excitation slits were set at 5 nm, and the scan rate was 240 nm/min. Fluorescence spectra of PS−C_{60} were measured at a series of concentrations to assign the emission wavelengths.

When a dilute PS solution is excited at $\lambda = 260$ nm, the fluorescence spectrum shows emissions from both the monomeric styrene unit and the intramolecular excimer at $\lambda = 285$ nm and $\lambda = 330-340$ nm, respectively.[12] Nongrafted C_{60} in solution at room temperature does not fluoresce at an excitation wavelength of 260 nm because of the highly symmetrical three-dimensional structure of C_{60}.[3] However, the fluorescence emission spectra of C_{60}-end-boned PS are quite different from those of bare C_{60}, PS, or the C_{60}−PS copolymer.[13]

Figure 2a shows the ratio of the fluorescence emission intensity with excitation at $\lambda = 260$ nm to a range of concentrations of C_{60}-*g*-PS in TCE. We observed that the shape and intensity of the peaks in the fluorescence emission spectra change over the concentration range of 0.02−0.03 g/L (Figure 2b). The significant decrease in fluorescence intensity from the monomers and excimers of C_{60}-*g*-PS can be attributed to quenching through intramolecular excited-state energy transfer, where the C_{60}-containing sites may act as energy traps.[14] Otherwise, C_{60}-*g*-PS displayed complicated emission peaks around $\lambda = 375$, 397, and 413 nm in TCE at room temperature. This may be a result of changes to the highly symmetrical shape of C_{60}.[3]

The fluorescence intensity, I, is related to the concentration, c, according to the following equation where I_0 is the intensity of the incident radiation,[15]

$$I = I_0(1 - e^{-abc})$$

The extinction coefficient is the variable a, and b is the path length of the cell. Figure 2b shows the change in the absolute intensity of emission at $\lambda = 397$ nm of C_{60}-*g*-PS as a function of concentration. It shows a linear dependence of $\ln(I/I_0)$ over the concentration range 0.02∼0.08 g/L, and the crossover concentration is about 0.1 g/L.

Table 1 summarizes the experimental parameters and results for the size measurements of the aggregates. The ratios of the

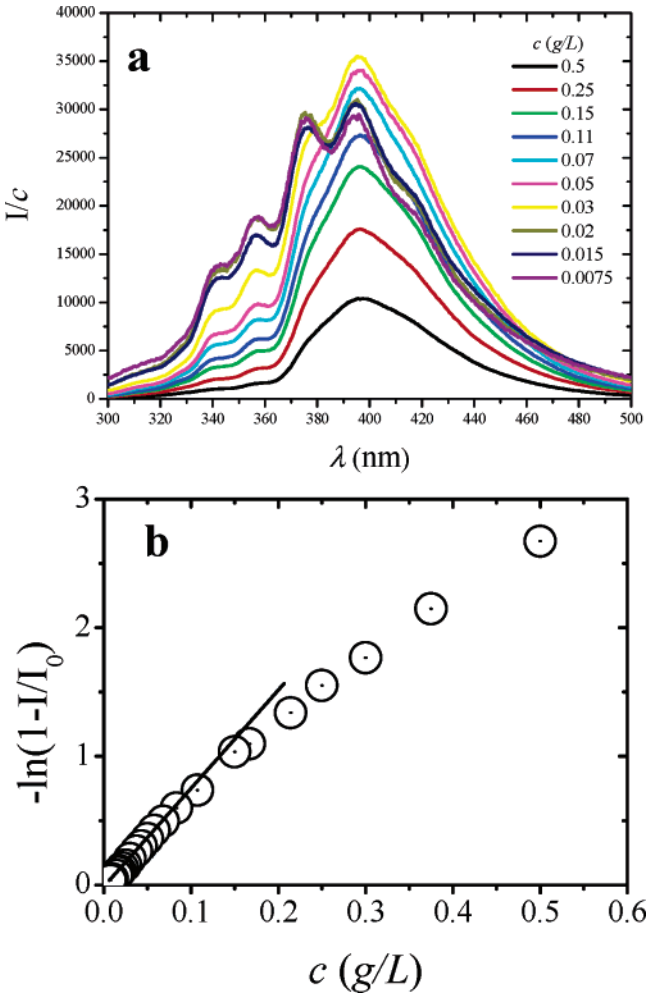

Figure 2. (a) Ratio of the fluorescence emission intensities to concentration as a function of wavelength for the PS-grafted fullerenes in TCE solutions. The concentrations are 0.5, 0.25, 0.15, 0.1, 0.07, 0.05, 0.03, 0.02, 0.015, and 0.0075 g/L from top to bottom. (b) The concentration dependence of the intensity at $\lambda = 397$ nm.

TABLE 1: Parameters of Aggregates Formed from Polymer-Substituted Fullerenes

	C_{60}-*g*-PS	C_{60}-*g*-PMMA	C_{60}-*g*-PEO
M_w, g/mol	7900[a]	11 000[b]	2000
solvent	TCE	THF	water
concentration,[c] g/mL	1.56×10^{-4}	9.36×10^{-5}	5.86×10^{-5}
R_h, nm	113	70	48
$\langle R_{AFM} \rangle$, nm	60[c]	51	22
$\langle H_{AFM} \rangle$, nm	5.6	10	6.0
$\langle H_{AFM} \rangle / \langle R_{AFM} \rangle$	0.093	0.196	0.273
solubility of C_{60}, g/dm^3	0.16[d] (chloroform)	0.009	

[a] GPC results from ref 3. [b] GPC results from ref 6. [c] The R_h are obtained from the corresponding solution concentrations. The AFM samples were sprayed on a fresh mica surface from the same solution concentration. The samples were dried in a vacuum for 72 h prior to obtaining AFM images. [d] Reference 21 and references therein.

height to the radius, $\langle H_{AFM} \rangle / \langle R_{AFM} \rangle$, and the solubility of C_{60} is also listed for comparison.

3. Results and Discussion

Wang and co-worker's DLS results[6] describe two important characteristics of the C_{60}-grafted polymers in solution: (1) single-chain polymers as well as large aggregates were detected by DLS; and (2) the aggregate size decreased as the solution concentration increased. A simple micelle-like structure was supposed by Wang et al. to explain the size of aggregates observed by DLS qualitatively, as shown in Figure 3b. However, a detailed analysis shows that such a micelle-like model could not give a satisfactory prediction on the size of the aggregates in the solution and the concentration dependence of the size mentioned above. The size of a simple micelle should be on the same order of the free-grafted fullerene (Figure 3a), around several nanometers, which is contradictory to our experimental observation that a much larger size of aggregates (about 50−100 nm) are found in the solution. It is also clear that the simple micelle model could not predict the aggregate size decreases with the concentration increases. Thus, a description based on a simple micelle structure without the pure C_{60} core could not provide a convincing explanation of the size and concentration dependence of R_h. The vesicle model, which asks for the ratio of the radius of gyration to R_h to approach unity, is not successful at describing the aggregate structure of the grafted fullerene in solution.[10−11]

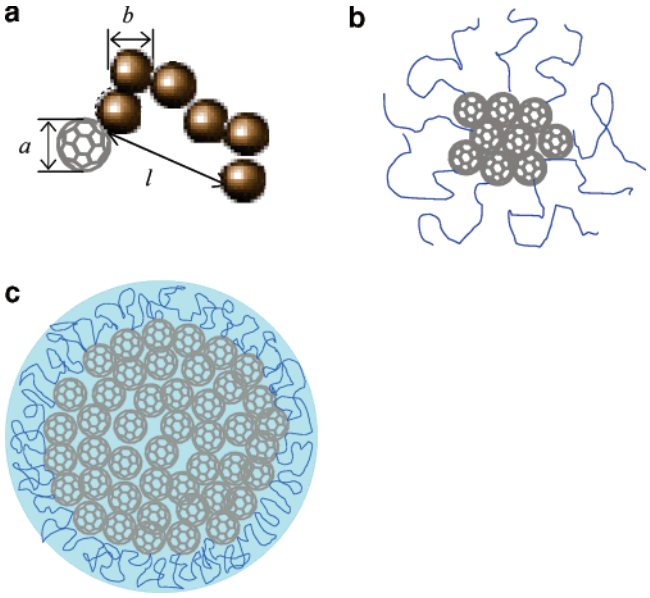

Figure 3. Schematic of the aggregate structure formed in a polymer-grafted fullerene solution. (a) A free-grafted fullerene in solution. (b) The simple micelle model suggested by Wang et al.[6] (c) The aggregates consist of pure fullerene molecules emulsified by the polymer-grafted fullerenes. The polymer-grafted fullerenes in solution and in the micelles are under dynamic equilibrium.

To explain the apparent contradiction, it is necessary to review the typical synthesis procedure for singly polymer-grafted fullerenes[3] from a reaction kinetics point of view. The graft reaction was performed in chlorobenzene at a temperature of approximately 100 °C with a feed mole ratio of 2:1 for C_{60} and the polymer. The reacted product was purified by dissolution in THF and reprecipitated by the addition of methanol. We emphasize that C_{60} is not very soluble in chlorobenzene and may form large aggregates in solution. As the reaction proceeds, the polymers cover the surface of the C_{60} particles. The reaction is terminated when the C_{60} surface is no longer polymer-accessible. Because of the small size of fullerene compared with that of the polymer chain length, the normal dissolution/reprecipitation method does not remove pure fullerenes that are stabilized by the polymer surfactant. Not only do the grafted fullerenes remain in the reaction mixture, but a large fraction of pure fullerenes are also present in the product. Many authors have reported a wide distribution of molecular weights from

GPC,[3−5] suggesting that the products are mixtures even after purification. The aggregates of emulsified fullerenes (Figure 3c) are reformed when the product is redissolved.

However, if we consider a solution of emulsified micelles, as shown in Figure 3c, the results of Wang and co-worker's[6] DLS experiments can be easily explained: the pure fullerenes are distributed in the solution stabilized by the grafted fullerenes in the form of emulsified micelle, where lots of free-grafted fullerenes are dissolved in the solution and, with an increase in concentration, more free-grafted fullerenes would enter the micelles, given that the concentration is above the critical micelle concentration (CMC). The emulsified micelles will split into smaller micelles to minimize the total free energy. We have developed a scaling argument to predict the concentration dependence on the aggregate size in the appendix of this paper. The simple scaling argument presented here is basically identical to the analysis of micelles formed by diblock copolymers[16−21] if we treat the fullerenes functionalized by flexible chains as the headgroup of a diblock polymer.

The polymer-substituted fullerene is considered a spherical particle with radius a grafted with a single polymer chain with n monomers (Figure 3a). For simplicity, monomers are assumed to have the same length, b, with the monomer being highly soluble in the solvent, while the particle is poorly soluble. The equilibrium size, l, of a free-grafted fullerene can be estimated from the balance of the two free-energy terms. In the limit of $d/R \ll 1$, the size of the emulsified micelle is related to the mole fraction of the grafted fullerene in an emulsified micelle, p, the size of the free-grafted fullerene, l, the reduced temperature, τ, the Boltzmann constant, k, the absolute temperature, T, and the elastic energy of the polymer chain at its equilibrium length, ϵ, by (see the appendix for details)

$$R \approx a\tau^{1/15}p^{-1}\left(\frac{kT}{\epsilon}\right)^{3/5}\left(\frac{a}{l}\right)^{4/5} \propto n^{-3/5} \propto M_w^{-3/5} \qquad (1)$$

Our scaling argument predicts that when the molecular weight is larger than $n_0 \approx \nu^{-2/3}a^{-2}b^4\tau^2$ (where ν is the exclude volume of the monomers), the size distribution of the aggregates narrows sharply, as observed in Figure 1a. The molecular-weight dependence is related to the ratio of d/R. As predicted by eq 1, the size decreases with the chain length, n, or molecular weight M_w for $d/R \ll 1$ and scales as $M_w^{-3/5}$. When the molecular weight is smaller than n_0, we predict that the size is independent of M_w, because the micelle could not be stabilized by the grafted fullerene and the size is controlled by the accessible surface area of the aggregate with a broad distribution. Based on our scaling argument, PS−C_{60} solutions with $M_w = 2700$ and 4700 g/mol are probably below the critical molecular weight and do not form stable structures. However, the sample with $M_w =$ 7900 g/mol could form self-assembled structures with narrow distributions.

We can relate the mole fraction of grafted fullerenes, q, in solution and the total mole concentration, c, of fullerenes by a simple phase-separation argument. Suppose that the solution separates into two phases, one phase consisting of free-grafted polymers in solution and an emulsified-micelle phase. Our theoretical calculation shows that the concentration dependence of the micelle size can be written in the limit of $d/R \ll 1$ as (see appendix for details)

$$R = R_0 q\left(1 + \frac{1-q}{q - c_0/c}\right) \qquad (2)$$

We fit Wang and co-worker's data[6] using eq 2 and show the results in Figure 4. The solid lines in Figure 4 correspond to eq 2 in which the CMC, c_0, the mole fraction of grafted fullerenes, q, and the micelle size at reference concentration, R_0, are considered to be adjustable parameters. As one can see from Figure 4, the lines corresponding to the theoretically predicted concentration dependence (eq 2) are in excellent agreement with the experimental points for AB50F and the higher concentration range of AM50F. The fitting results also show that the CMC, c_0, is about 0.1 g/L, which is consistent with a crossover of the fluorescence emission intensities shown in Figure 2. The most dilute point of AM50F is out of our prediction curve and is attributed to the instability of the emulsified micelles in the concentration range close to the CMC.

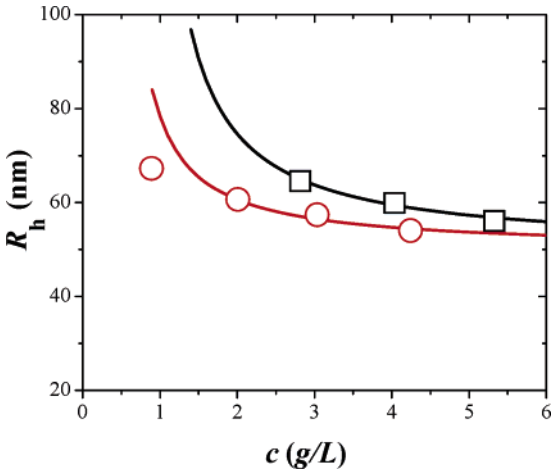

Figure 4. Concentration dependence of the aggregate size: fullerenes grafted by PMMA in THF (AM50F, square), fullerenes grafted by poly(*n*-butyl methacrylate) in THF (AB50F, circle).[6] The fitting parameters of the solid lines given by eq 2 are $R_0 = 50$ nm, $q = 0.15$, and $c_0 = 0.08$ g/L for AM50F and $R_0 = 50$ nm, $q = 0.15$, and $c_0 = 0.11$ g/L for AB50F.

The AFM images also confirm our findings, although the AFM images only show the aggregate pattern at the surface. As summarized in Table 1, the volume of the particles is proportional to the R_h observed by DLS in solution. We can imagine that the particles are formed as the solvent evaporates, therefore, the height of the particles would decrease as drying time increases. If C_{60} is more hydrophobic than the solvent, there will be a lower concentration of the solvent in the core of aggregates, meaning that the ratio $\langle H_{AFM}\rangle/\langle R_{AFM}\rangle$ should increase as the solubility of C_{60} increases. We observed that the volume of the PS−C_{60} particles at the mica surface decreases after storage in air for one month, while PMMA−C_{60} and PEO−C_{60} samples are almost unchanged.

4. Conclusions

We have analyzed the self-organized supermolecular architectures of singly polymer-substituted fullerenes observed in solution by light scattering and fluorescence spectroscopy, as well as the surface pattern obtained when the aggregates were sprayed from the solution by AFM. We predict that there is a critical molecular weight that yields a narrow distribution of self-assembled structures.

Acknowledgment. We appreciate C. Wu and F. Li for providing the polymer-grafted C_{60} samples for the study. This work is supported by NFSC Grant Nos. 20474075 and 20490220, by Innovation Funding No. KJCX2-SW-H07 from Chinese Academy of Sciences, and 973 Grant No. 2003CB615604 from Chinese Ministry of Science and Technology.

Appendix

A.1. Size of a Free-Grafted Fullerene. We model the solution as a ternary mixture of pure fullerenes, grafted fullerenes, and solvents, in which the all-pure fullerenes are emulsified and stabilized by the grafted fullerenes above CMC, because of its poor solubility, where the free-grafted fullerenes are dissolved in the solution. The polymer-substituted fullerene is considered a spherical particle with radius a grafted with a single polymer chain with n monomers (Figure 3a). For simplicity, monomers are assumed to have the same length, b, with the monomer being highly soluble in the solvent, while the particle is poorly soluble. The equilibrium size, l, of a free-grafted fullerene can be estimated from the balance of the two free-energy terms. The first term is due to the two-body repulse interaction, and the second one is the elastic energy of a strand with n monomers. (We ignore all numerical prefactors of unity below.)

$$F \approx kT\nu\frac{n^2}{l^3} + kT\frac{l^2}{nb^2} \tag{A1}$$

In eq A1, k is the Boltzmann constant, T is the temperature, and ν is the excluded volume of the monomers. In the Flory notation,[17] $\nu = (1 - 2\chi)b^3 = (T - \Theta_p/T)b^3$, where χ is an interaction parameter and Θ_p is the theta temperature for the polymer in solution. For a good solvent, $0 < \nu < 1/2$ and $\Theta_p < T$. The length of the polymer tail is determined by the minimization of the free energy in eq A1

$$l \approx \nu^{1/5}b^{2/5}n^{3/5} \tag{A2}$$

The corresponding elastic energy of the polymer chain at its equilibrium length, l, is

$$\epsilon \approx kT\nu^{2/5}b^{-6/5}n^{1/5} \tag{A3}$$

A.2. Size of an Emulsified Micelle. Let us first consider an emulsified micelle with a core of m pure fullerenes, which are stabilized by s grafted fullerenes, as shown in Figure 3c. The size of the fullerene core is determined by the balance between the two-body attraction interaction and the three-body repulsive interaction:

$$F_{\text{core}} \approx -kTa^3\tau\frac{(s+m)^2}{R^3} + kTa^6\frac{(s+m)^3}{R^6} \tag{A4}$$

where $\tau = (\Theta_f - T)/\Theta_f$ is the reduced temperature for the fullerenes in the core and $\Theta_f > T$ for the poor solubility of the fullerenes. The core size, R, is

$$R \approx a\tau^{-1/3}(s+m)^{1/3} \tag{A5}$$

and the minimum energy of F_{core} (eq A4) is

$$F_{\text{core}} \approx -kT\tau^2(s+m) \tag{A6}$$

The optimal size of such a micelle is determined by the interplay between the surface energy of the core of the micelle composed of the fullerene and the repulsive interaction of the excluded volume in the corona.

The size of the core R affects the surface energy in the following manner:

$$F_s \approx \gamma R^2 \approx \gamma a^2\tau^{-2/3}(s+m)^{2/3} \approx kT\tau^{4/3}(s+m)^{2/3} \tag{A7}$$

where the surface tension can be defined as $\gamma \approx kT\tau^2/a^2$. The optimal size of the micelle corona d can be estimated by minimizing the free energy of the corona

$$F_{\text{corona}} \approx kT\nu\frac{(sn)^2}{(R+d)^3 - R^3} + kTs\frac{d^2}{nb^2} \tag{A8}$$

The first term of eq A8 is the repulsion energy of the excluded volume, and the second term is the entropy cost due to the stretching of the polymer chain. The minimization of the free energy of corona (eq A8) leads to an optimal corona size

$$d \approx \begin{cases} ls^{1/5}, & \text{for } d \geq R \\ l^{5/3}s^{1/3}R^{-2/3}, & \text{for } d \ll R \end{cases} \tag{A9}$$

Substituting the optional corona size (eq A9) into the expression of the corona free energy (eq A8), the free energy of the corona at equilibrium with $(s + m)$ fullerenes per micelle is

$$F_{\text{corona}} \approx \begin{cases} s^{7/5}\epsilon, & \text{for } d > R \\ s^{5/3}\left(\frac{l}{R}\right)^{4/3}\epsilon, & \text{for } d \ll R \end{cases} \tag{A10}$$

The optimal aggregation number $(s + m)$ of C_{60} is obtained by minimizing the chemical potential of the micelle $\mu = \partial(F_{\text{corona}} + F_s)/\partial(s + m)$ that results from the following expressions when the number fraction of the grafted fullerenes $p = s/(s + m)$ in an emulsified micelle is fixed:

$$s + m = \frac{s}{p} \approx \begin{cases} p^{-21/11}\left(\frac{kT}{\epsilon}\right)^{15/11}\tau^{20/11}, & \text{for } d \geq R \\ p^{-3}\left(\frac{kT}{\epsilon}\right)^{9/5}\left(\frac{a}{l}\right)^{12/5}\tau^{8/5}, & \text{for } d \ll R \end{cases} \tag{A11}$$

The size of the aggregates is given by eq A9 and A11 when $d \geq R$ and by eq A5 and A11 when $d \ll R$:

$$R \approx \begin{cases} \tau^{4/11}p^{-2/11}\left(\frac{kT}{\epsilon}\right)^{3/11}l \sim n^{6/11}, & \text{for } d \geq R \\ a\tau^{1/15}p^{-1}\left(\frac{kT}{\epsilon}\right)^{3/5}\left(\frac{a}{l}\right)^{4/5} \sim \mathrm{n}^{-3/5}, & \text{for } d \ll R \end{cases} \tag{A12}$$

A.3. Critical Molecular Weight. The number of fullerenes in one micelle is constrained by the surface area of the core. With an increased number of fullerenes in the core, the micelle is destabilized if the grafted chain is not in contact with the solvent. In other words, the fullerene cannot enter the core when the surface area of core is smaller than the sum of the cross section of the chain. Therefore, the following condition must be met to obtain stable aggregates with s grafted fullerenes:

$$R^2 \geq sb^2 \tag{A13}$$

Substituting eq A5 and A11 into eq A13 yields,

$$s \leq (a/b)^6\tau^{-2}p^{-2} \tag{A14}$$

When $d \ll R$, the critical molecular weight of the polymer n_0 should be

$$n \geq n_0 \approx \nu^{-2/3}a^{-2}b^4\tau^2 \tag{A15}$$

A.4. Concentration Dependence of the Emulsified Micelle. We can relate the fraction of grafted fullerenes, $p = s/(m + s)$, in an emulsified micelle and the total mole concentration, $c =$

$(m + s + k)/V$, of fullerenes in solution by a simple phase-separation argument (where k is the mole number of free-grafted fullerenes in the solution, and V is the volume of solution averaged for one aggregate). Suppose that the solution separates into two phases, one phase consisting of free-grafted polymers in solution and an emulsified micelle phase. Assuming there is phase equilibrium between the free-grafted fullerenes in solution and the grafted fullerenes at the micelle surface,

$$\frac{s+k}{m} = \frac{1}{q^{-1}-1} = \frac{1}{p^{-1}-1} + \frac{c_0}{(1-q)c} \qquad \text{(A16)}$$

where the total mole fraction of grafted fullerenes is $q = (s + k)/(m + s + k)$ and $c_0 \approx (k/V)$ is the mole concentration of the grafted polymer in the solution phase, if the solution is dilute. Substituting eq A16 into the expression of the size of the emulsified micelle (eq A12), the concentration dependence of the micelle size can be written in the approximation of $d \ll R$ as

$$R = R_0 q\left(1 + \frac{1-q}{q - c_0/c}\right) \qquad \text{(A17)}$$

References and Notes

(1) Diederich, F.; Thilgen, C. *Science* **1996**, *271*, 317 and references therein.

(2) Okamura, H.; Ide, N.; Minoda, M.; Komatsu, K.; Fukuda, T. *Macromolecules* **1998**, *31*, 1859.

(3) Zhou, P.; Chen, G.; Hong, H.; Du, F.; Li, Z.; Li, F. *Macromolecules* **2000**, *33*, 1948.

(4) Yang, J.; Li, L.; Wang, C. *Macromolecules* **2003**, *36*, 6060.

(5) Huang, X. D.; Goh, H. *Macromolecules* **2000**, *33*, 8894.

(6) Wang, X.; Goh, H.; Lu, Z. H.; Lee, S. Y.; Wu, C. *Macromolecules* **1999**, *32*, 2786.

(7) Song, T.; Dai, S.; Tam, K. C.; Lee, S. Y.; Goh, S. H. *Langmuir* **2003**, *19*, 4798.

(8) Jeng, U.-S.; Lin, T.-L.; Tsao, C.-S.; Lee, C.-H.; Canteenwala, T.; Wang, L. Y.; Chiang, L. Y.; Han, C. C. *J. Phys. Chem. B* **1999**, *103*, 1059.

(9) Hernandez, M.; Monroy, F.; Ortega, F.; Rubio, R. G. *Langmuir* **2001**, *17*, 3317.

(10) Antonietti, M.; Stephan, F. *Adv. Mater.* **2003**, *15*, 1323.

(11) Zhou, S.; Burger, C.; Chu, B.; Sawamura, M.; Nagahama, N.; Toganoh, M.; Hackler, U.; Isobe, H.; Nakamura, E. S*cience* **2001**, *291*, 1944.

(12) Morawetz, H. *Science* **1979**, *203*, 405.

(13) Bunker, C. E.; Lawson, G. E.; Sun, Y. P. *Macromolecules* **1995**, *28*, 3744.

(14) Guillet, J. E. *Polymer photophysics and Photochemistry*; Cambridge University Press: New York, 1985.

(15) Ranby, B.; Rabek, J. F. *Photodegragation, Photooxidation and Photostabilittion of polymers*; John Wiley and Sons: London, 1975.

(16) Flory, P. J. *Principles of Polymer Chemistry*; Cornell University Press: Ithaca, NY, 1953.

(17) de Gennes, P.-G. *Scaling Concepts in Polymer Physics*; Cornell University Press: Ithaca, NY, 1979.

(18) Izzo, D.; Marques, C. M. *Macromolecules* **1993**, *26*, 7189.

(19) Pepin, M. P.; Whitmore, M. D. *Macromolecules* **2000**, *33*, 8654.

(20) Marques, C.; Joanny, J. F.; Leibler, L. *Macromolecules* **1988**, *21*, 1051.

(21) Alargova, R. G.; Deguchi, S.; Tsujii, K. *J. Am. Chem. Soc.* **2001**, *123*, 10460.